Deeper insight into Gambierdiscus polynesiensis toxin production relies on specific optimization of High-Performance Liquid Chromatography High Resolution Mass Spectrometry

Thomas Yon, Manoella Sibat, Damien Réveillon, Samuel Bertrand, Mireille Chinain, Philipp Hess

Talanta
September 2021, Volume 232, Pages 122400 (11p.)
https://doi.org/10.1016/j.talanta.2021.122400
https://archimer.ifremer.fr/doc/00689/80147/

Deeper insight into *Gambierdiscus polynesiensis* toxin production relies on specific optimization of High-Performance Liquid Chromatography High Resolution Mass Spectrometry

Yon Thomas [1, *], Sibat Manoella [1], Réveillon Damien [1], Bertrand Samuel [2, 3], Chinain Mireille [4], Hess Philipp [1]

[1] IFREMER, DYNECO, Laboratoire Phycotoxines, F-44000 Nantes, France
[2] Université de Nantes, MMS, EA 2160, Nantes, France
[3] ThalassOMICS Metabolomics Facility, Plateforme Corsaire, Biogenouest, Nantes, France
[4] Institut Louis Malardé, UMR 241 EIO, 98713 Papeete, Tahiti, French Polynesia

* Corresponding author : Thomas Yon, email address : Thomas.yon@ifremer.fr

Abstract :

Ciguatera food poisoning affects consumer health and fisheries' economies worldwide in tropical zones, and specifically in the Pacific area. The wide variety of ciguatoxins bio-accumulated in fish or shellfish responsible for this neurological illness are produced by marine dinoflagellates of the genus Gambierdiscus and bio-transformed trough the food web. The evaluation of the contents of ciguatoxins in strains of Gambierdiscus relies on the availability of standards and on the development of sensitive and specific tools to detect them. There is a need for sensitive methods for the analysis of pacific ciguatoxins with high resolution mass spectrometry to ensure unequivocal identification of all congeners. We have applied a fractional factorial design of experiment 2^8-3 for the screening of the significance of eight parameters potentially influencing ionization and ion transmission and their interactions to evaluate the behavior of sodium adducts, protonated molecules and first water losses of CTX4A/B, CTX3B/C, 2-OH-CTX3C and 44-methylgambierone on a Q-TOF equipment. The four parameters that allowed to significantly increase the peak areas of ciguatoxins and gambierones (up to a factor ten) were the capillary voltage, the sheath gas temperature, the ion funnel low pressure voltage and the ion funnel exit voltage. The optimized method was applied to revisit the toxin profile of G. polynesiensis (strain TB92) with a confirmation of the presence of M-seco-CTX4A only putatively reported so far and the detection of an isomer of CTX4A. The improvement in toxin detection also allowed to obtain informative high resolution targeted MS/MS spectra revealing high similarity in fragmentation patterns between putative isomer (4) of CTX3C, 2-OH-CTX3C and CTX3B on one side and between CTX4A, M-seco-CTX4A and the putative isomer on the other side suggesting a relation of constitutional isomerism between them for both isomers.

Graphical abstract

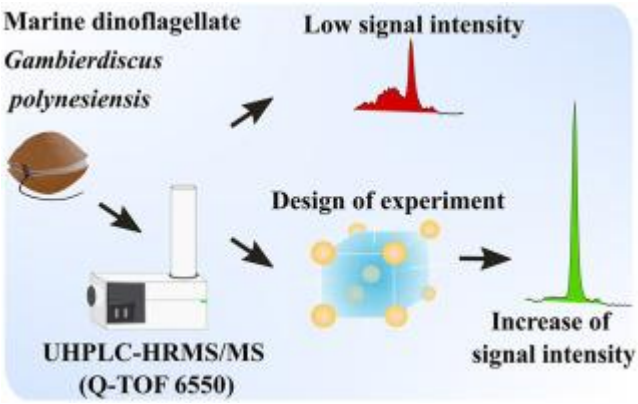

Highlights:

► A chemometric method to weigh the contribution of Q-TOF parameters is proposed. ► Ionization and transmission parameter increased sensitivity for ciguatoxin analysis. ► M-*seco*-P-CTX4A is a major ciguatoxin produced by G. polynesiensis. ► Putatively reported “isomer (4) of P-CTX3C” is a constitutional isomer.

Keywords : Mass spectrometry, *Gambierdiscus polynesiensis*, ciguatoxins, gambierones, Fractional Factorial Design

1. Introduction

Ciguatera is the largest non-bacterial foodborne illness affecting more than 50 000 people annually with gastric, cardiac and neurological symptoms [1] . Initially discovered in tropical and sub-tropical areas, occurrence of the disease appears to increase due to climate and other environmental changes as well as the expansion of international tourism and trade, see Chinain et al, [2,3] for a review and references therein. This neurological illness affects humans within a few hours and can last up to several months after the consumption of shellfish or fish contaminated *via* feeding either directly on marine ciguatoxin (CTX)-producing dinoflagellates from the genera *Gambierdiscus* and *Fukuyoa*, or indirectly *via* accumulation in the food chain of carnivore organisms [1,4].

More than 12 different species of *Gambierdiscus* and *Fukuyoa* have been reported with high variation of ciguatoxin-like toxicity from fg to pg equivalent CTX3C $cell^{-1}$ (Longo et al., and references therein) [5-9]. However the result obtained by bioassays (e.g. mouse-bioassay, cell-based bioassay, receptor-binding assay) largely depended on the sample preparation, the complexity of matrix effect and the detection method. To date, only *Gambierdiscus polynesiensis* reported by Chinain et al., [10] has been unequivocally confirmed as a ciguatoxin producer by analytical tools, i.e. mass spectrometry (MS) and nuclear magnetic resonance spectroscopy (NMR spectroscopy)[10-13].

Other species such as *G. australes, G. belizeanus* and *G. excentricus* were demonstrated as producers of maitotoxins [6,14-17], *G. toxicus* produced gambieric acids [18,19], gambieroxide [20] and gambierol [21], and finally gambierones [22-24] were reported in 16

73 species of *Gambierdiscus* and recently also in 2 species of *Fukuyoa* and 2 species of *Coolia*
74 [8,25-27].

75 Ciguatoxins are lipophilic polyethers (octanol-water partition coefficients (XlogP3-AA)
76 ranging from 2.5 to 4.7) [28] with a mass ranging from 1000 to 1200 Da. Four types of
77 structure have been described so far according to their carbon skeleton and origin, i.e. P-CTX
78 I (i.e. CTX4A type) and II (i.e. CTX3C type) (Figure 1) both found in the Pacific Ocean,
79 Caribbean-CTX (C-CTX) in the Caribbean area and Indian-CTX (I-CTX) in the Indian
80 Ocean. [29,30].

81 The complex toxin profile of *G. polynesiensis* has so far mostly been evaluated with low
82 resolution mass spectrometry and contains more than 12 analogs of ciguatoxins (Figure 1),
83 [8,11,31-35].

84

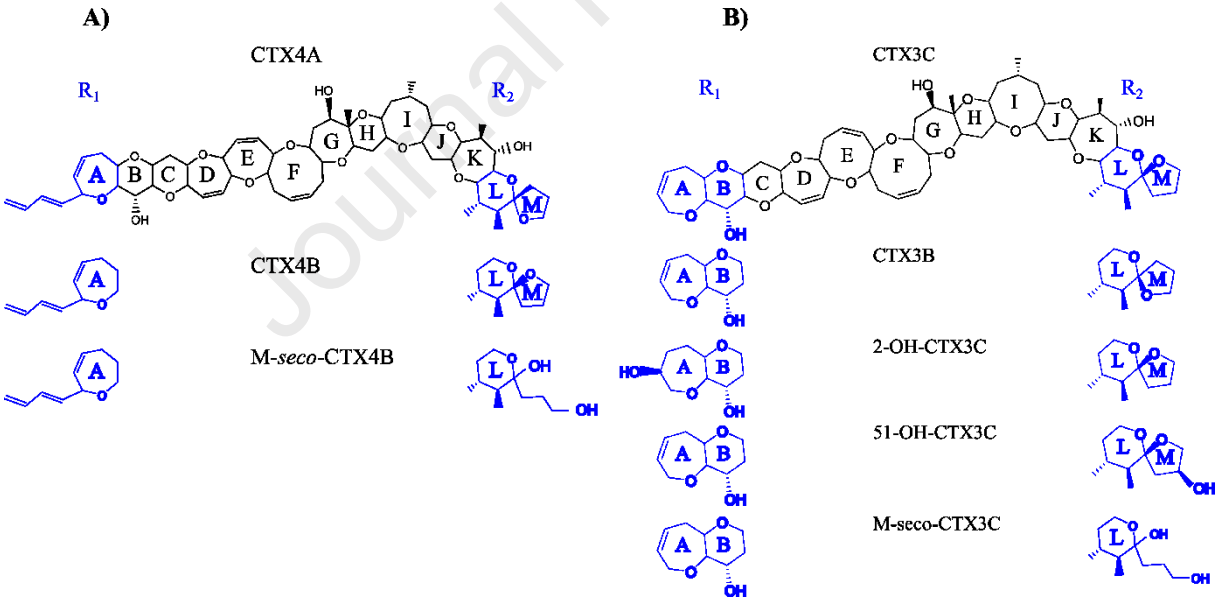

85

86 **Figure 1.** Reported structure of Pacific Ciguatoxins produced by *G. polynesiensis* according to the type of
87 structure: A) CTX4A group and B) CTX3C group [36] (no structure is known for the four isomers of CTX3C)

88

89 In addition to ciguatoxins, *G. polynesiensis* was also reported as producer of gambierone
90 and its analog 44-methyl gambierone [8,37-39]. The *G. polynesiensis* strain TB92 was used as

a "reference material" in many studies (e.g. [32,34,37,40]) focusing on its toxin profile and the modifications that may occur throughout the food web.

The low number of strong acidic or basic functional groups in algal ciguatoxins appears to result in low ionization yield in electrospray type source, thus raising the detection limits compared to many other algal-derived polyethers [41]. However, the use of MRM mode operated in tandem mass spectrometers allows to focus on a limited number of compounds and thus, achieves relatively low limits of detection for ciguatoxins in fish or algal extracts (1-2 ng mL^{-1}) [34,42]. A major drawback of the MRM mode is that it requires knowledge on the mass spectral behavior of compounds to define the transitions monitored (precursor/product ion pairs) and their ion ratio. So far, only two standards of CTX are commercially available and thus, quantitative estimation of concentrations were typically carried out by assuming equal response factors with CTX1B or CTX3C and results were commonly expressed as CTX1B or CTX3C equivalents [41].

An alternative to confirm the presence of known compounds or to detect related, unknown compounds in complex extracts is high-resolution mass spectrometry (HRMS) [34,41]. With hybrid high resolution systems such as quadrupole-time-of-flight (Q-TOF) technology, both targeted and untargeted analyses can be performed allowing for retrospective data analysis [43,44]. Compared to MRM mode performed in tandem mass spectrometry (i.e. triple quadrupole or Q-Trap), the full scan acquisition carried out on a Q-TOF mass spectrometer suffers from a 10 to 12 times lower sensitivity [34]. To overcome the sensitivity issue, a rigorous optimization of the ionization and transmission parameters is required to detect trace amounts of CTXs. So far, such optimization of ciguatoxin detection was only performed with low resolution mass spectrometry, using either one parameter at the time or multiple parameters with an experimental design [34,42,45]. Chemometric optimization of ion funnel parameters has already been proven to efficiently increase peak

area of urine metabolites [46]. In this study, a fractional factorial design of experiment (FFD) was used on a Q-TOF, equipped with the dual ion funnel technology to evaluate the significance of 8 electrospray ionization and ion transmission parameters on the chromatographic peak area obtained for ciguatoxins and gambierones present in methanolic extracts of *G. polynesiensis* strain TB92. Improving the detection of polyethers while enhancing the formation of protonated ions are key objectives to obtain intense and informative MS/MS spectra for ciguatoxins. Optimal values for significant parameters were implemented and allowed us to describe the toxin profile of *G. polynesiensis* with HRMS and notably the presence of M-*seco*-CTX4A that was only putatively reported so far. The increase of peak area of CTX3B/C by a factor five resulting from the optimization enabled the acquisition of targeted HRMS/MS spectra of CTX3B and isomer (4) of CTX3C confirming the constitutional isomerism between the two compounds.

2. Materials and Methods

2.1. Chemicals

LC–MS grade methanol, formic acid (98% purity) and ammonium formate were purchased from Sigma Aldrich (Saint Quentin Fallavier, France). Water was deionized and purified at 18 MΩ cm thanks to a Milli-Q integral 3 system (Millipore, France).

For HRMS, acetonitrile, methanol and high purity water were purchased from Optima Fisher chemical (Illkirch, France).

A mix of ciguatoxin standards (M-*seco*-CTX3C, 2-OH-CTX3C, 51-OH-CTX3C, CTX2, CTX3B, CTX3C, CTX4A and CTX4B) was provided by Dr. Mireille Chinain, Institut Louis Malardé (ILM), Tahiti, French Polynesia.

2.2. Sample preparation

Dried methanolic extracts corresponding to one million cells of *Gambierdiscus polynesiensis* TB92 (Tubuai, Australes archipelago, French Polynesia) were prepared at Institut Louis Malardé (ILM), Tahiti, French Polynesia using the same procedure as published in Chinain et al., [11]. Briefly, fresh cell pellet was extracted twice with 20 mL of methanol 100% and twice with 20 mL of aqueous methanol 50% under sonication for 10 min each. Supernatants were obtained after centrifugation at 2800g for 10 min, pooled and evaporated.

Two dried extracts corresponding to 1.7 x 10^6 and 1 x 10^6 cells equivalent/mL were resuspended each in 1 mL of methanol, filtered through 0.25 µm GF/F filters (Whatman, France) and were used for the design of experiment and the toxin profile assessment, respectively.

2.3. Instrumental conditions for the design of experiment

Analyses were carried out using a system composed of ultra-high performance liquid chromatography UHPLC (1290 Infinity II, Agilent Technologies, CA, USA) coupled to a 6550 ion funnel Q-TOF (Agilent Technologies, CA, USA) equipped with a Dual Jet Stream® ESI source. The nebulizer was set at 35 Psi in agreement with Agilent recommendation for a flow rate of 0.4 mL min^{-1} and the sheath gas flow (SGF) varied according to the sheath gas temperature (SGT) (5, 6 and 11 L min^{-1} for 250, 325 and 400 °C, respectively). All other source and transmission parameters varied as described in the fractional factorial design (see section 2.5 and Figure 2).

The instrument was operated in full scan positive mode, at a scan rate of 2 spectra s^{-1} over a mass-to-charge ratio (*m/z*) from 100 to 1700. Reference mass *m/z* 922.0099 (hexakis phosphazene) was injected continuously over the entire run to ensure no deviation in mass measurement.

Instrument control and data treatment were carried out using the MassHunter software version B.08 (Agilent Technologies, CA, USA) and peaks were integrated using the algorithm

164 Agile2 of the Mass Hunter Qualitative Analysis software. The chromatographic method was
165 adapted from Sibat et al., [34]. Briefly, the stationary phase was a Kinetex C18 column (50 x
166 2.1 mm, 1.7 µm 100 Å, Phenomenex, CA, USA) maintained at 40 °C. The mobile phases
167 were 100% water (eluent A) and acetonitrile/water (95:5, v/v) (eluent B), both contained 2
168 mM ammonium formate and 50 mM formic acid. The flow rate was 0.4 mL min^{-1} and the
169 elution gradient was as follows: 10% to 95% of B from 0 to 12 min, held at 95 % B for 2 min
170 and then return to initial condition (10 %B) at 14.1 min and held for 6 min.
171 The chromatographic conditions used in this study allowed the detection of a wide variety of
172 compounds including ciguatoxins, maitotoxins and gambierones. To reduce the number of
173 experiments, the detection of ciguatoxins and gambierones was achieved simultaneously,
174 resulting in the coelution of CTX3B with 3C and CTX4A with 4B.
175 Conditions were randomized in the run sequence and experimental blanks were added
176 between two different conditions to avoid any cross-contamination and ensure the stability
177 (i.e. temperature) between each condition. Triplicate injections under the same conditions
178 were, however, performed successively to reduce the equilibration time.
179 Finally, the average of the peak area of the extracted ion chromatogram (EIC) was
180 selected as the response for each toxin and ion species (Table 1).

181 **Table 1.** Toxin, retention time and selected ion species (accurate mono isotopic *m/z*) for the fractional factorial
182 design of experiment (RT = retention time)

Toxin	**Molecular Formula**	**RT (min)**	**$[M-H_2O+H]^+$ (*m/z*)**	**$[M+H]^+$ (*m/z*)**	**$[M+Na]^+$ (*m/z*)**
44-methylgambierone	$C_{51}H_{76}O_{19}S$	7.5	1021.4825	1039.4931	1061.4750*
2-OH-CTX3C	$C_{57}H_{84}O_{17}$	9.1	1023.5676	1041.5781*	1063.5601
CTX3C and 3B	$C_{57}H_{82}O_{16}$	11.8	1005.5570	1023.5676	1045.5495
CTX4A and 4B	$C_{60}H_{84}O_{16}$	12.4	1043.5726	1061.5832	1083.5652

183 *Ions excluded from the FFD as they were not detected in the majority of the runs

2.4. Fractional Factorial Design (FFD) of experiment

A fractional factorial design (FFD) (2_{IV}^{8-3}) with a resolution of 4 was selected for the investigation of the direct effects of 8 factors and their interactions (order 2). An FFD can only evaluate the significance of the effects (i.e. contribution) of factors and the level giving the best response among the experimental domain considered (i.e. either -1 or +1 level for each factor).

The selection of significant factors and their interactions was performed assuming that interactions between three or more factors were supposed as negligible and the interaction between non-significant factors were considered as non-significant and thus removed from the results.

Statgraphics Centurion 18 (Version 18.1.02) was used for the experimental design and the statistical analysis.

For the ion funnel Q-TOF (Figure 2), the ionization and transmission parameters are separated into two categories: flow-dependent (nebulizer pressure (NP), drying gas temperature (DGT) and flow (DGF), sheath gas flow (SGF)) and compound-dependent (capillary voltage (CV), nozzle voltage (N), ion funnel voltages (high pressure (IFHP), low pressure (IFLP) and exit (IFE) direct current), sheath gas temperature (SGT) and fragmentor voltage (FV)) [47]. The parameters which can be set in the system (the IFHP and IFLP) are time-varying potentials used to compress the ion beam and improve the transmission. The dual ion funnel technology first removes the gas and neutral noise with radio frequency applied in the IFHP, then focuses the ion beam to the center in the IFLP and finally the direct current (DC) voltage applied in the IFE accelerates the ions (Figure 2) [48].

The 8 factors used in the FFD were selected using Agilent recommendations [47] for compound-dependent parameters. The levels were defined either by the limit of the instrument for the high level, or by selecting the lowest value allowing to detect the reference

mass *m/z* 922.0099 (hexakis phosphazene). Levels of the 8 factors (low [-1], center [0] and high [+1] values) are summarized in Figure 2 and the matrix corresponding to the 32 experiments is provided in Table S1.

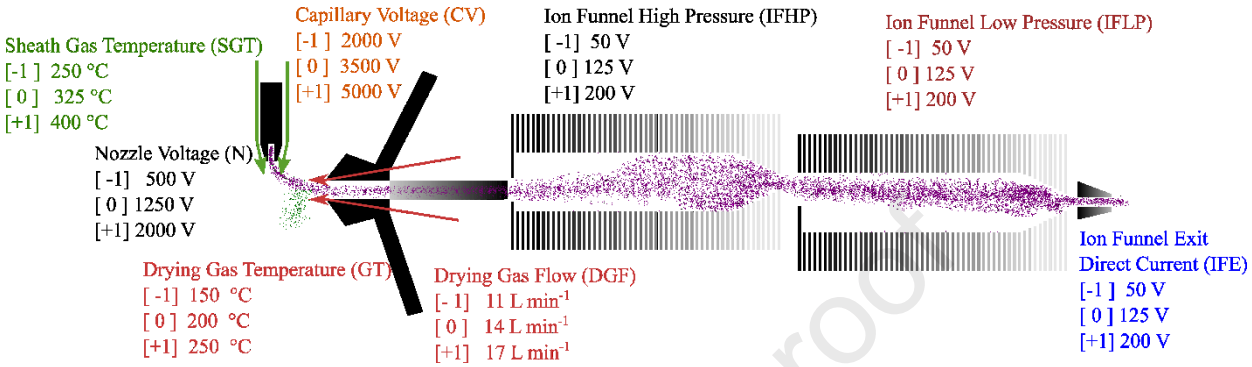

Figure 2. Scheme of Agilent Q-TOF 6550 electrospray source and dual ion funnel with the parameters (factors) and their levels (low [-1], center [0] and high [+1]) used in the fractional factorial design

LC-HRMS systems can provide accurate masses but suffer from low sensitivity. As the only commercial standard of ciguatoxin (CTX3C, Wako, Tokyo, Japan) is limited by cost and availability, it was not possible to optimize MS parameters using this standard. Alternatively, and to account for matrix effect and the possible divergence of responses between ciguatoxin analogs, we used an extract of *G. polynesiensis* (strain TB92 estimated as 5.8 ± 0.85 pg CTX3C equivalent $cell^{-1}$ [32]) corresponding to 1.7 million cells (*i.e.* 10 µg mL^{-1} of ciguatoxins (sum of CTX3B/C and 4A/B)), making this sample highly suitable for this HRMS optimization.

The peak area corresponding to the ion $[M+H-H_2O]^+$, $[M+H]^+$ and $[M+Na]^+$ of each compound was log(10) normalized before statistical analyses. The protonated molecule $[M+H]^+$ of 2-OH-CTX3C and the sodium adduct $[M+Na]^+$ of 44-methylgambierone were excluded from the FFD as they were detected in only few conditions. When no peak was detected, the value was set as half of the average noise (*i.e.* 100).

For all responses, an ANOVA was performed to test the statistical significance of each effect at a level of confidence of 95% comparing the least square against the estimation of the experimental error. A Durbin-Watson test assessing the correlation between the residuals values and the order of experiment was performed to ensure at a level of confidence of 95% that the residuals were not correlated to the order of injections.

2.5. Instrumental conditions for the toxin profile of *G. polynesiensis*

For the revisit of the toxin profile of *G. polynesiensis,* two chromatographic methods were used. For gambierones, the chromatographic method was the same as used for the FFD as it allowed to separate gambierone from 44-methylgambierone. For ciguatoxins, the chromatographic method used in the FFD was not able to separate related compounds (i.e. CTX3B from CTX3C), hence, and to facilitate comparison with the literature, we used a chromatographic method already published by Sibat et al., [34], the "LC method n°2". Shortly, a linear gradient using water 100% as eluent A and methanol 100% as eluent B both containing 2 mM of ammonium formate and 50 mM of formic acid was used on a Zorbax Eclipse Plus C18 column (50 × 2.1 mm, 1.8 µm, 95 Å, Agilent Technologies, Santa Clara, CA, USA). The elution gradient started at 78% of B then rose up to 88% of B in 10 min and held for 4 min before the reconditioning for 5 min. The flow rate was 0.4 mL min^{-1}, the column was maintained at 40 °C and the injection volume was 5 µL.

Peak area and signal-to-noise ratio (S/N) were obtained using MassHunter algorithm for Extracted Ion Chromatogram (EIC) of the ions presented in Table 2 with a delta ppm tolerance of 10.

For structural comparison between CTX3B, the isomer (4) of CTX3C and 2-OH-CTX3C on one side and CTX4A, M-s*eco*-CTX4A and the isomer of CTX4A on the other side, mass spectra were acquired by targeted MS/MS over a *m/z* range of 50-1300 at 10 spectra s^{-1} for MS and 3 spectra s^{-1} for MS/MS levels. Three collision energies were used (10, 20 and 40

255 eV). Instrument control and data treatment were carried out using the MassHunter software
256 version B.08 and B.07 (Agilent Technologies, CA, USA).
257

258 **Table 2.** Toxin, retention time and selected ion species (accurate mono isotopic *m/z*) for toxin profile

	Toxin	**Retention Time (min)**	**$[M-H_2O+H]^+$ (*m/z*)**	**$[M+H]^+$ (*m/z*)**	**$[M+NH_4]^+$ (*m/z*)**
Method gambierones	gambierone	7.4	1007.4669	1025.4774	1042.5040
	44-methylgambierone	7.6	1021.4825	1039.4931	1056.5196
Method CTXs	2-OH-CTX3C	3.9	1023.5676	1041.5781	1058.6047
	M-*seco*-CTX4A	5.2	1061.5832	1079.5938	1096.6203
	Isomer (4) of CTX3C	8.7	1005.5570	1023.5676	1040.5941
	CTX3B	9.6	1005.5570	1023.5676	1040.5941
	CTX3C	9.8	1005.5570	1023.5676	1040.5941
	Isomer of CTX4A	9.8	1043.5726	1061.5832	1078.6098
	CTX4A	10.7	1043.5726	1061.5832	1078.6098
	CTX4B	11.2	1043.5726	1061.5832	1078.6098

259

260 # 3. Results and discussion

261 ## 3.1. Significance of the factors

262 The FFD allowed to assess the contribution (or weight) of the eight factors on the peak
263 area of the ten selected response providing information about in-source fragmentation, adduct
264 formation as well as protonated molecule ionization and transmission.

265 The peak areas of all ion species (Table S2) showed high variations and ranged from 100
266 (undetected) to 4 x 10^6 counts depending on the conditions. The significant factors at a
267 confidence level of 95 % (*p*-values from 0.05 to 0.0001) and their contribution on the

responses are presented in Figure 3. The variability explained by the model was excellent (R^2 ranged from 85% to 97%).

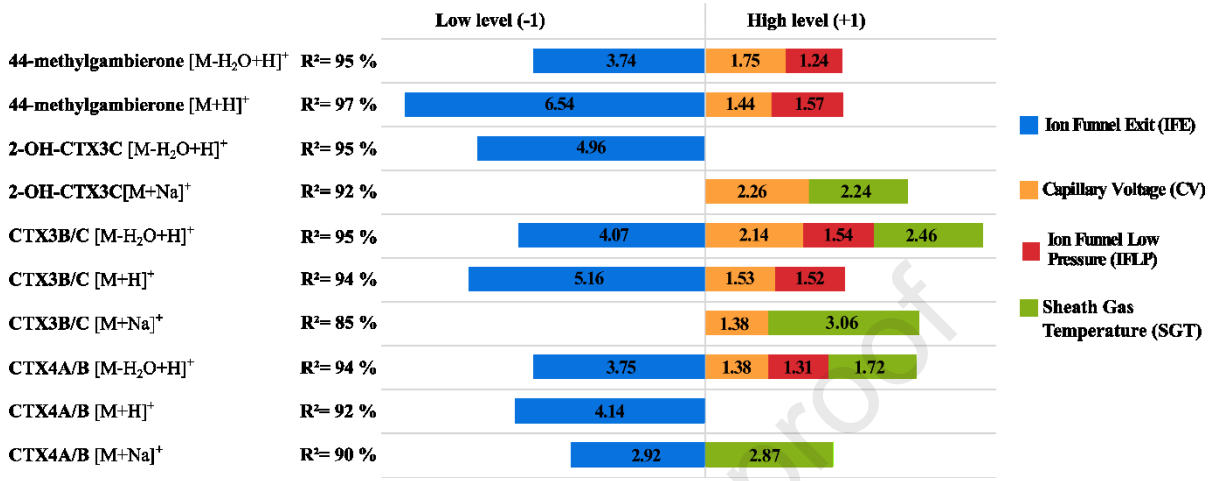

Figure 3. Combined Pareto chart with the contribution (bar size) and levels (-1 or +1) of all significant (at a confidence level of 95 %) factors on the responses, and percentage of variability explained by the model (R^2)

The most influent parameters (*i.e.* with the highest contribution) were the CV, the SGT, the IFLP and the IFE (Figure 3).

Therefore, among the ionization parameters, the increase of the CV significantly enhanced the areas of CTXs and 44-methylgambierone. The SGT when set at high level (*i.e.* 400°C) appeared to increase the first water loss and sodium adduct formation of CTXs while all other parameters (N, DGT and DGF) were not significant (p-value > 0.05).

The CV increases the number of charges available for the ionization and the SGT improves the desolvation of compound and removes noise. The results are in agreement with Yogi et al., [45] and Mead et al., [49] suggesting that the electrospray ionization of such polyethers with very low number of ionizable groups (i.e. acidic or basic functional groups) can be challenging and requires stronger conditions. Our results also demonstrated that none of the ionization parameters could selectively increase the protonated molecular ion without

increasing the first water loss or the sodium adduct and thus, it is recommended to set a high value of CV and SGT to increase the ionization yield.

The dual ion funnel technology was implemented in the Q-TOF 6550 to overcome the difficulties of controlling the ion motion in presence of strong gas dynamics and thus to increase the ion transmission [47,50]. Among ion transmission parameters, the IFLP and IFE voltages were significant at a confidence level of 95% whereas the IFHP voltage was not significant. Consistent results were also reported by Peris-Diaz et al., [46] on the same analytical system. A lower value of voltage applied in the IFE resulted in an increase of the transmission of the protonated molecule and first water loss ions of all polyethers (Figure 3). This observation suggests that ions may be fragmented or poorly transmitted in the ion funnel if they are exceedingly accelerated by the IFE voltage [48]. Noteworthy, the first water loss ion did not increase when IFE parameter was set at mid or high level (*i.e.* 125 or 200 V, respectively) revealing that this water loss is more likely to appear in the electrospray source rather than into the ion funnel.

However, when we observed a significant effect of the IFLP factor (mostly for $[M-H_2O+H]^+$ and $[M+H]^+$ ions) the best response was obtained with the higher level (*i.e.* 200 V) suggesting that these ions still needed high voltage to be efficiently focused.

The sodium adduct formation was increased by either a high value of CV and SGT or a low value of IFE for all responses, as those parameters increased also the protonated molecule and the first water loss, none of the conditions studied could reduce significantly the adduct formation.

Hence, we recommend to use the IFLP at high level (*i.e.* 200 V) and the IFE at low level (*i.e.* 50V) to enhance the overall sensitivity for the Q-TOF detection of polyethers from *Gambierdiscus*.

The FFD provided the significance and the contribution of the ionization and transmission parameters on the responses with a limited number of experiments compared to a full factorial design. Here, with only 133 injections corresponding to 44 h of chromatographic run time (one blank and a triplicate of injection for each condition) instead of 1024 injections (*i.e.* 14 d and 5 h of chromatographic run time) for a full factorial design, four parameters were clearly demonstrated as significant to increase the peak area of CTXs and 44-methylgambierone. This approach could have been strengthened using a second design of experiment focusing on the four key parameters with more than 2 levels. However, these results already highlighted the behavior of sodium adducts, protonated molecules and first water loss ions according to the different factors tested. It should be noted that the significant parameters were all compound-dependent and thus, should improve the ionization and transmission of ions independently of the mobile phase used.

3.2. Signal enhancement

Q-TOF type systems can perform targeted MS/MS that relies on the fragmentation of selected precursor ions in the collision chamber to obtain the fragments (*i.e.* product ions) and gain insight into structural information. As demonstrated for other types of polyethers [51], the presence of sodium adducts can dramatically reduce the degree of fragmentation in the CID chamber compared to the protonated molecule. It is therefore critical to use parameters that favor the protonated molecules without increasing the in-source fragmentation or sodium adduct formation to achieve a higher sensitivity.

Accordingly, the parameters of the run n°17 and n°31 used in the FFD (Table S2 and S3) were chosen for subsequent analyses of CTXs and gambierones respectively, and compared to the previous “in house” method used in the laboratory (derived from “LC method 3” in Sibat et al., [34]). The peak area of each protonated molecule is presented in Figure 4 and details of the ionization and transmission parameters for the three methods can be found in Table S3.

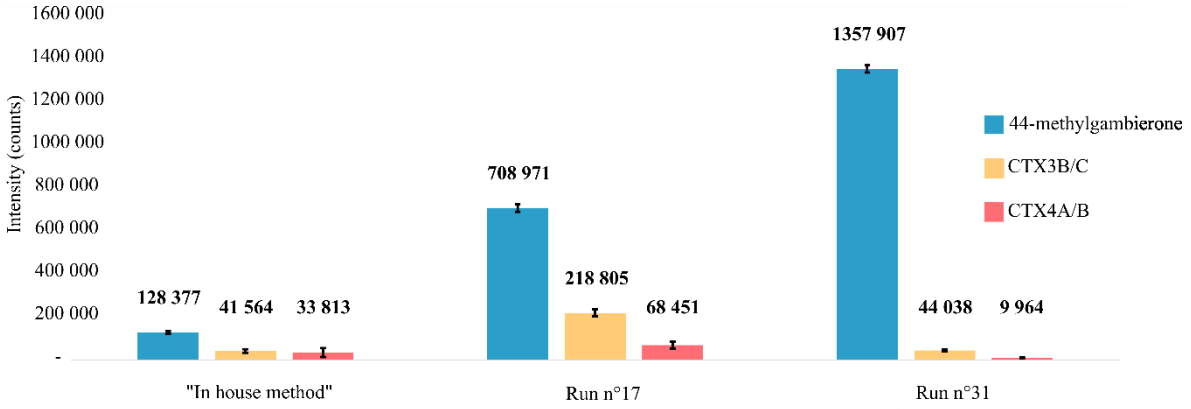

Figure 4. Peak area of Extract Ion Chromatograms (tolerance ± 10 ppm) of protonated molecules of 44-methylgambierone, CTX3B/C and CTX4A/B from full scans acquired with ESI+ LC-HRMS using the parameters of the "In house method", run n°17 and run n°31 (Table S3).

When using optimized parameters, the average peak area (triplicate of injection) of the $[M+H]^+$ ion of 44-methylgambierone was increased by a factor 10 compared to the method previously used in the laboratory (Figure 4). Similarly, for ciguatoxins, peak areas were increased by a factor 5 and 2 for CTX3B/C and CTX4A/B, respectively.

As reflected by Figure 4 and Figure S1, ionization and transmission parameters can significantly change the relative toxin profile observed here on a sample of *G. polynesiensis* strain TB92, highlighting the necessity to optimize HRMS parameters to lower the limits of detection of gambierones and ciguatoxins on a Q-TOF system. When focusing only on gambierones, the parameters used for the run n°31 are thus recommended. However, as the peak area for 44-methylgambierone was always more than 3 times higher than the one of CTX3B/C and CTX4A/B, for the subsequent analyses the parameters increasing CTX areas were considered as more important than those increasing only the area of gambierones.

3.3. Toxin profile of *G. polynesiensis* TB92

355 So far, the toxin profile of TB92 had only been explored with low resolution mass
356 spectrometry, using the MRM mode of acquisition with two or three transitions per toxin
357 [11,34,38,40,52]. The identity was confirmed by the comparison of transitions, ion ratio and
358 retention time with purified CTX standards. Further identifications were achieved based on
359 literature information using identical chromatographic methods as reported and comparing the
360 retention order, in addition to retention time and tandem-MS spectrum. A major issue with
361 this approach was the misidentification of unknown ciguatoxins, when the retention time was
362 unknown and the transitions were unspecific. For example, the signal observed for the
363 transition $[M+H]^+/[M-H_2O+H]^+$ of CTX3B/C could be attributed to either a new CTX3B/C
364 analog or to the transition $[M-H_2O+H]^+/[M-2H_2O+H]^+$ of a hydroxylated analog that
365 underwent an in-source water loss. In this study, the use of HRMS in Full Scan mode
366 followed by a targeted MS/MS on unknown compound was performed in order to provide a
367 complete picture of the different form of ions corresponding to gambierones and CTXs in *G.*
368 *polynesiensis* TB92 including adduct formation protonated molecule or even in-source water
369 loss.

370 **3.3.1. Gambierones**

371 The peak area of 44-methylgambierone was 50 times higher than gambierone (Figure 5)
372 and the detection of gambierone here was only possible thanks to the significant enhancement
373 of signal resulting from the previous optimization.

374

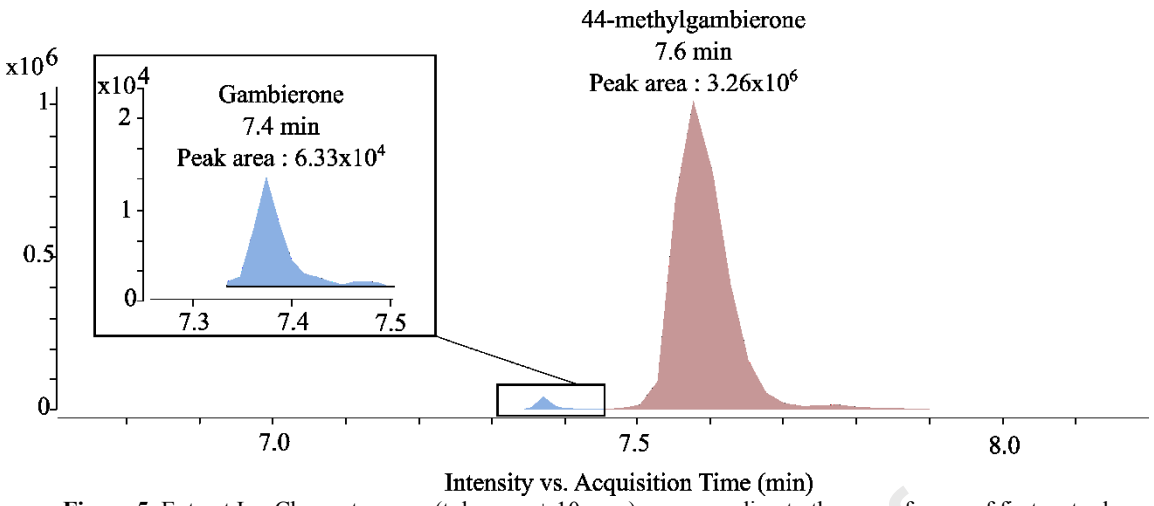

Figure 5. Extract Ion Chromatograms (tolerance ± 10 ppm) corresponding to the sum of areas of first water loss, protonated molecule and ammonium adduct of gambierone and 44-methylgambierone from full scan acquired with ESI+ LC-HRMS.

The ubiquitous presence of gambierone and 44-methylgambierone in four *G. polynesiensis* clones has recently been reported [8,33]. Initially found in *G. belizeanus* [22,23], gambierone and 44-methylgambierone now seem to be common to 16 species of *Gambierdiscus,* 2 species of *Fukuyoa* and 2 species of *Coolia* [16,25,26]. To date, only *G. excentricus* was not demonstrated as a gambierone or 44-methylgambierone producer but interestingly, this species produced a compound responding to the transition *m/z* 1037/97 but with a different retention time [16]. In addition, *G. jejuensis* has not been tested for the presence of gambierone analogs yet [53].

The quantitative profile of gambierones in *G. polynesiensis* has been described for four mono-clonal strains, by comparing the exponential and stationary growth phases and the intracellular/extracellular proportions [8]. The cell quotas were strain-dependent but gambierone was always produced in higher amount than 44-methylgambierone with a difference ranging from 2 to 7.5-fold. For this sample (*G. polynesiensis* strains TB92), the 44-methylgambierone is clearly the major product with an abundance 50 times higher than

gambierone. This difference can be attributed to either strain variability or method for extraction and storage.

3.3.2. Ciguatoxins

LC-HRMS analysis of the methanolic extract of the *G. polynesiensis* strain TB 92 demonstrated the presence of eight CTX analogs (Figure 6), namely 2-OH-CTX3C, M-*seco*-CTX4A, isomer (4) of CTX3C, CTX3B, CTX3C, an isomer of CTX4A, CTX4A and CTX4B.

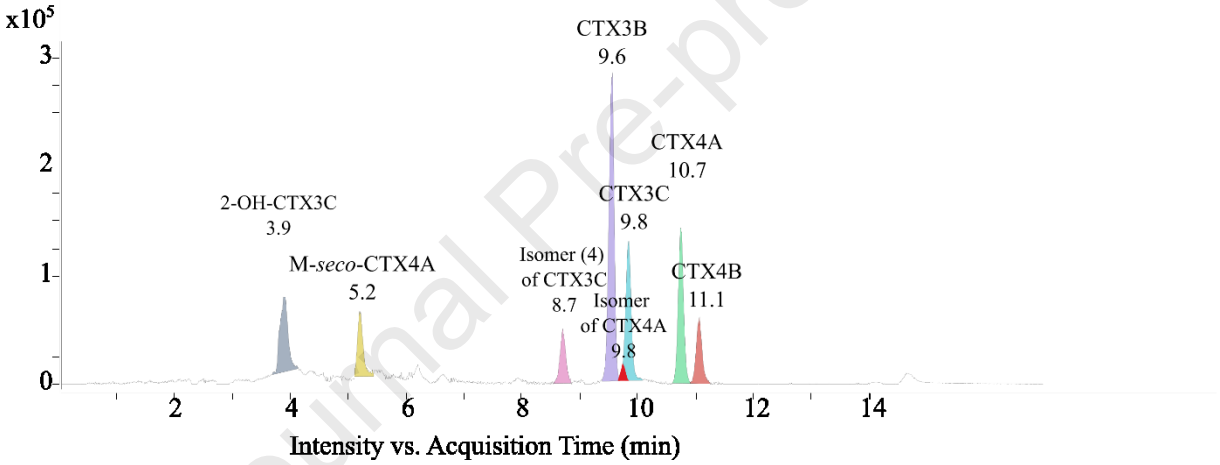

Figure 6. Extract Ion Chromatograms (tolerance ± 10 ppm) corresponding to the sum of areas of first water loss, protonated molecule and ammonium adduct ions of CTXs from full scan acquired with ESI+ LC-HRMS.

Reliable identification of the toxin congeners was carried out on the full scan analysis based on mass and spectral accuracy for the first water loss, the protonated molecule and the ammonium or sodium adduct (details provided in Figures S3-to-S10). In addition, the toxin profile obtained by low resolution mass spectrometry in MRM mode acquired with the method published in Sibat et al., [34] was compared to the mix of CTXs standard available from ILM (detail provided in Figure S2). The toxin profile obtained was rather consistent with previous studies on *G. polynesiensis* strains [8,11,32-34,38,40]. In recent studies, four CTX3C-like compounds (*i.e.* peak responding to at least two transitions of CTX3C in MRM

mode but with a different retention time) that were identified as potential isomers according to their elution order in reversed phase chromatography, have been reported in *G. polynesiensis* [8,34,38,40] with retention times between M-*seco*-CTX3C and CTX3B. No structural information is available for these isomers as they never had been isolated and analyzed either by HRMS or NMR spectroscopy.

In this study, due to a still lower sensitivity of the Q-TOF compared to a hybrid quadrupole ion-trap mass spectrometer operating in MRM mode [34,38], only the isomer (4) of CTX3C (*i.e*. the most intense) was detected at a retention time of 8.7 min while M-*seco*-CTX3C and 3-OH-CTX3C were not detected.

In contrast to gambierone and 44-methylgambierone, the variation of ciguatoxin profile of *G. polynesiensis* strain TB92 since the first description in 2010 by Chinain et al., [11] was low. The major toxin produced is still CTX3B, followed by CTX3C and CTX4A and B and then 2-OH-CTX3C, M-*seco*-CTX4A and the presence of CTX3C isomers is consistent with the intensities reported previously [33,34,40].

The low difference in retention time between CTX3B and the isomer (4) of CTX3C (0.9 min) suggested a high structural similarity. In contrast, the hydroxylated form of CTX3C (2-OH-CTX3C), also produced by *G. polynesiensis,* eluted at 3.9 min (*i.e*. 5.7 min earlier than CTX3B), this high difference in retention time suggested that the isomer (4) was more closely related to CTX3B or C than to a hydroxylated form of CTX3B/C. To obtain more insights into the structure of the isomer (4) of CTX3C, targeted HRMS/MS spectrum was obtained on the *m/z* 1005.5570 as it was the most abundant ion found in the full scan spectra (Figures S3,5,6).

3.3.3. Isomer (4) of CTX3C

Some parts of the fragmentation pattern of CTX3C were described in previous studies [11,34,41] (Figure 7A in blue). In this study, the fragmentation pattern of the epimer of

CTX3C (CTX3B) was acquired as the chromatographic peak was more intense (Figure 6) but both compounds share the same spectrum (as expected since the only structural difference is in the stereochemistry of the L- and M- rings). The reported fragmentation pathway was characterized by a succession of water losses from *m/z* 1023.5541 ($[M+H]^+$) to *m/z* 933.5084 ($[M-5H_2O+H]^+$) corresponding to the successive dehydration on B-, G- and K- ring followed by the opening and water losses occurring on L- and M- ring. The opening of the L-ring resulted also in the formation of *m/z* 907.4838. The opening of the G- to H-ring followed by several water losses was observed with the cluster from *m/z* 465.2847 to 411.2530 for the H- to M-side of the molecule and with the *m/z* 541.2796 (water loss originated from the *m/z* 559) for the A- to G-side of the molecule. The opening of K-, L- and M-rings resulted in five characteristic small ions: *m/z* 155.1071, 125.0960, 99.0807, 71.0491 and 59.0491.

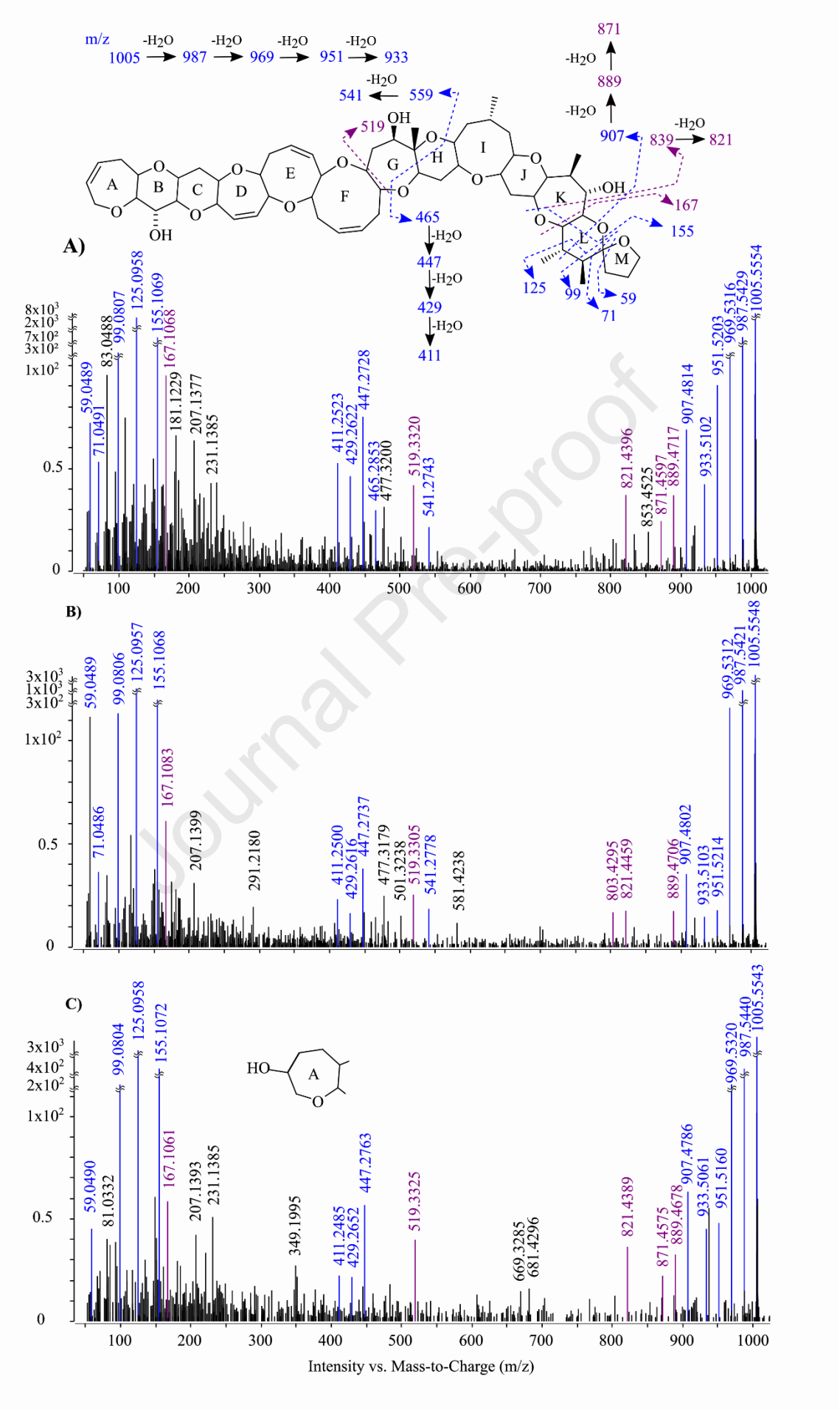

Figure 7. Fragmentation pathways based on HRMS/MS spectra obtained on Q-TOF by targeted MS/MS (average of three collision energies 10, 20 and 40 eV) on the precursor ions *m/z* 1005.5570 for chromatographic peak corresponding to A) CTX3B, B) Isomer (4) of CTX3C and C) 2-OH-CTX3C. Described in literature (in blue) and proposed (in purple).

The high concentration of CTX3B present in the sample associated with the improvement of ionization and transmission from the source to the analyzer of both protonated molecule and first water loss contributed to the observation of hitherto unreported fragments in the spectrum (Figure 7A in purple). The molecular formula of these ions and the associated errors are presented in Table 3. The attribution of the fragments was carried out using the "molecular formula analysis" provided by Chemcalc (https://www.chemcalc.org/) [54] with an error of less than 5 ppm in mass accuracy associated with the number of unsaturations. Hence, we report that the opening of the L-ring in our condition was followed by two water losses *m/z* 889.4733 (-1.8 ppm) and *m/z* 871.4627 (-3.4 ppm). Additionally, the opening of the K-ring (*m/z* 839.4576 not observed) was followed by one water loss *m/z* 821.4471 (-4.3 ppm). Fragmentation of the G-ring resulted in the formation of *m/z* 519.3316 (+0.8 ppm). For the small fragments, the opening of the K-ring produced *m/z* 167.1067 (+0.6 ppm).

Table 3. Ion species corresponding to the accurate mono-isotopic *m/z* of CTX3B, isomer (4) of CTX3C and 2-OH-CTX3C. Mass differences (Δppm) were compared between theoretical exact mass and measured *m/z*.

Ion Formula	Theoretical mono isotopic mass (Da)	NI*	CTX3B	Δ ppm	Isomer (4) of CTX3C	Δ ppm	2 OH-CTX3C	Δ ppm
$[C_{57}H_{81}O_{15}]^+$	1005.5570	18	1005.5554	-1.6	1005.5548	-2.2	1005.5543	-2.7
$[C_{57}H_{79}O_{14}]^+$	987.5464	19	987.5429	-3.5	987.5421	-4.4	987.544	-2.4
$[C_{57}H_{77}O_{13}]^+$	969.5359	20	969.5316	-4.4	969.5312	-4.8	969.532	-4.0
$[C_{57}H_{75}O_{12}]^+$	951.5253	21	951.5203	-5.3	951.5214	-4.1	951.516	-9.8
$[C_{57}H_{73}O_{11}]^+$	933.5147	22	933.5102	-4.8	933.5103	-4.7	933.5061	-9.2
$[C_{51}H_{71}O_{14}]^+$	907.4838	17	907.4817	-2.3	907.4802	-4.0	907.4786	-5.7
$[C_{51}H_{69}O_{13}]^+$	889.4733	18	889.4717	-1.8	889.4706	-3.0	889.4678	-6.2
$[C_{51}H_{67}O_{12}]^+$	871.4627	19	871.4597	-3.4			871.4575	-6.0
$[C_{47}H_{65}O_{13}]^+$	839.4576	15						
$[C_{47}H_{63}O_{12}]^+$	821.4471	16	821.4436	-4.3	821.4459	-1.5	821.4389	-10
$[C_{47}H_{61}O_{11}]^+$	803.4365	17			803.4295	-8.7		
$[C_{31}H_{41}O_8]^+$	541.2796	12	541.2743	-9.8	541.2778	-3.3		
$[C_{30}H_{47}O_7]^+$	519.3316	7.5	519.332	0.8	519.3305	-2.1	519.3325	1.7
$[C_{30}H_{45}O_6]^+$	501.3211	8.5			501.3238	5.4		
$[C_{26}H_{41}O_7]^+$	465.2847	7	465.2853	1.3	465.284	-1.5		
$[C_{26}H_{39}O_6]^+$	447.2741	8	447.2728	-2.9	447.2737	-0.9	447.2763	4.9
$[C_{26}H_{37}O_5]^+$	429.2636	9	429.2622	-3.3	429.2616	-4.7	429.2652	3.7
$[C_{26}H_{35}O_4]^+$	411.2530	10	411.2523		411.25	-7.3	411.2485	-11
$[C_{10}H_{15}O_2]^+$	167.1067	4	167.1068	0.6	167.1083	9.6	167.1061	-3.6
$[C_9H_{15}O_2]^+$	155.1067	2.5	155.1069	1.3	155.1068	0.6	155.1072	3.2
$[C_8H_{13}O]^+$	125.0961	2	125.0958	-2.4	125.0957	-3.2	125.0958	-2.4
$[C_6H_{11}O]^+$	99.0804	2	99.0807	3.0	99.0806	2.0	99.0804	0.0
$[C_4H_7O]^+$	71.0491	2	71.0491	0.0	71.0486	-7.0		
$[C_3H_7O]^+$	59.0491	1	59.0489	-3.4	59.0489	-3.4	59.049	-1.7

*NI: number of unsaturation

The fragmentation observed in this study as well as the pathways reported in the literature corresponded mainly to fragments resulting from opening of the cycles from the G- to M- side suggesting that A- to F- rings required higher collision energy to open.

The intensity of ions observed in the spectrum of CTX3B was two times higher than for isomer (4) or for 2-OH-CTX3C. Despite the variation in intensity, only small differences were observed in the fragmentation spectra when comparing CTX3B and 2-OH-CTX3C (Figure 7A and C). The precursor ion *m/z* 1005 used in this study corresponded to either $[M\text{-}H_2O+H]^+$ for isomer (4) and CTX3B or to $[M\text{-}2H_2O+H]^+$ for 2-OH-CTX3C, as one of these two water losses corresponded to the loss of the hydroxyl group on the A- ring, both the structure of 2-OH-CTX3C and CTX3B became identical after the rearrangement explaining the similarity in

fragmentation pathways. The opening of the G- and H-rings was not observed (*m/z* 541.2796) and other ions were observed with no clear correlation with the fragmentation pathway.

Isomer (4) of CTX3C previously reported by low resolution mass spectrometry [8,11,34,38,40] was only putatively characterized by SIM mode with the *m/z* 1023.8 and 1045.8 and by MRM mode using the transitions *m/z* 1040.6/1005.6, 1023.6/1005.6 and 1045.6/1045.6. The same compound was probably detected by Roué et al., [37]. In our study, we used HRMS and HRMS/MS to improve the mass accuracy of the ion measured compared to low resolution mass spectrometry. Firstly, the masses of the first water losses and the protonated molecule were highly accurate (error < 0.5 ppm) (Figure S6) showing that the molecular formula of this compound was $C_{57}H_{82}O_{16}$. Secondly, this compound showed a fragmentation pattern closely related to the one of CTX3B. The presence of *m/z* 541.2778 (-3.3 ppm) suggested that the A- to G- side of the molecule of this analog was common with CTX3B. The opening and water losses of the G- to M-ring of the molecule were the same as found for CTX3B too, hence no clear difference in structure was found. However, the similarity in terms of retention time with CTX3B compared to 2-OH-CTX3C (Figure 6) suggests that the difference between the isomer (4) of CTX3C and CTX3B was due to the change in the position of a methyl or a hydroxyl group along the carbon skeleton of the compound. Furthermore, as the stereochemical differences between CTXs congeners described in previous studies [31,36,55] were restricted to the orientation or configuration of the spiroketal L-, M- ring, the stereochemistry of other chiral centers could not be determined so a difference based in the position of the methyl or hydroxyl group remain possible.

3.3.4. M-*seco*-CTX4A and isomer of CTX4A

So far, the presence of M-*seco*-CTX4A at a significant amount (*i.e* peak area similar to 2-OH-CTX3C) was only putatively reported with low-resolution mass spectrometry in *G. polynesiensis* TB92 (*i.e*. without standard confirmation) by Chinain et al., [11] and Roué et al., [32]. A compound eluting earlier than CTX4A sharing the same MRM transitions as CTX4A was also reported by Murray et al., [33] in *G. polynesiensis* CAWD212. In this study, the presence of M-*seco*-CTX4A in *G. polynesiensis* TB92 was ascertained by mass and spectral accuracy (Figure S4) with an error less than 5 ppm for monoisotopic *m/z* corresponding to $[M\text{-}H_2O+H]^+$ (-0.4 ppm), $[M\text{-}H_2O+NH_4]^+$ (-4.7 ppm) and $[M+Na]^+$ (+0.3 ppm).

Furthermore, on the sum of EIC corresponding to the different form of ions (water loss, protonated molecule or adduct) observed for CTX4A and CTX4B, a small peak eluting at 9.8 min was also observed.

To obtain more information about M-*seco*-CTX4A and the putative isomer of CTX4A, targeted HRMS/MS spectrum was obtained on the *m/z* 1061.5833 (Figure 8) as it was the most abundant and common ion found in the full scan spectra of CTX4A, M-*seco*-CTX4A and the isomer of CTX4A(Figures S4, 8 and 9).

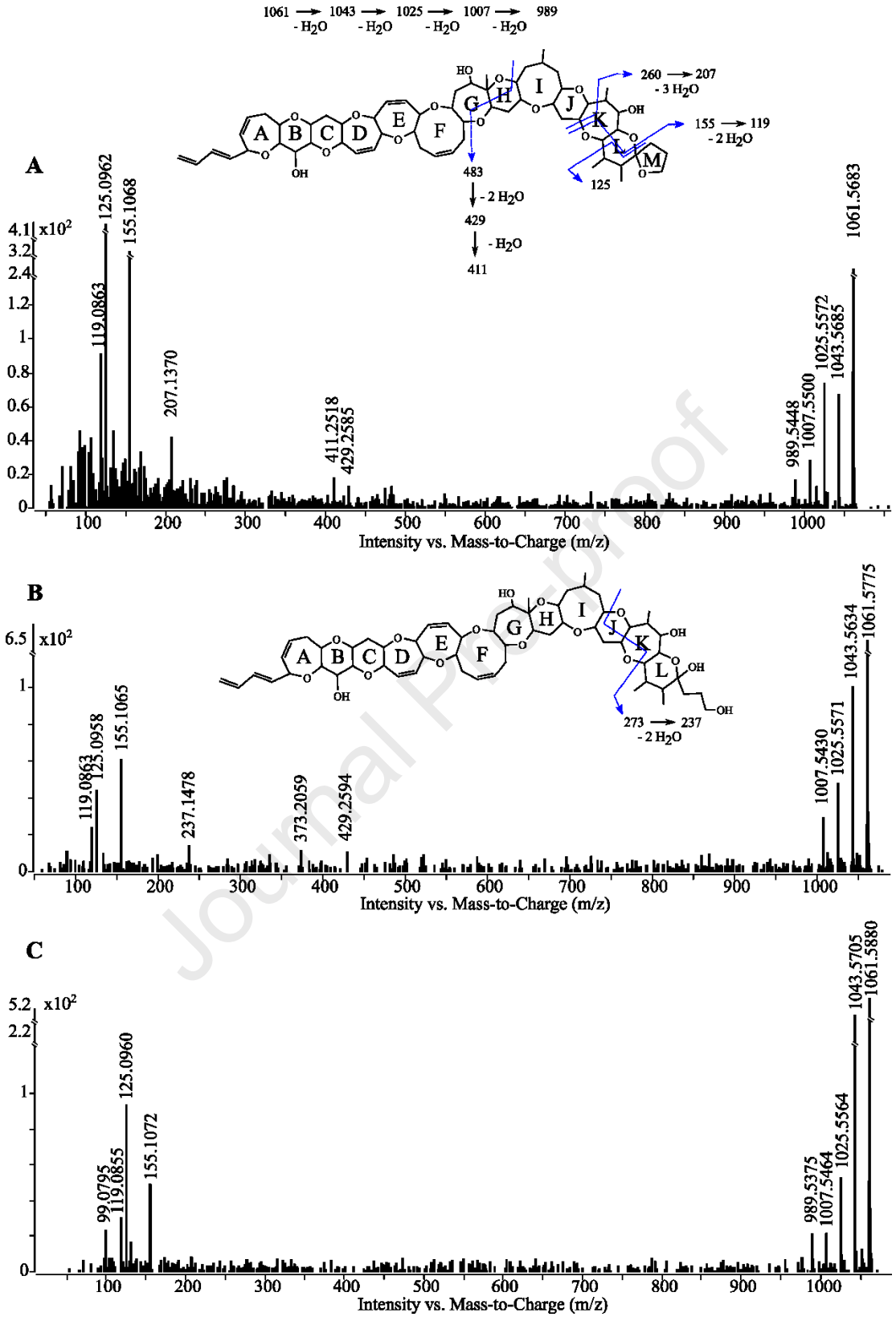

Figure 8. Proposed fragmentation pathways based on HRMS/MS spectra obtained by targeted MS/MS on the precursor ions *m/z* 1061.5833 for chromatographic peak corresponding to A) CTX4A at eluting at 10.8 min (with a collision energy of 40 eV), B) M-*seco*-CTX4A at 5.2 min (collision energy 20 eV) and C) a potential isomer of CTX4A at 9.8 min (collision energy 20 eV)

The fragmentation pattern of CTX4A type share similarity with the CTX3C type such as the succession of four water losses from *m/z* 1061.5833 to *m/z* 989.541 corresponding to the successive dehydration on B-, G- and K- ring followed by opening and a water loss of L- ring (Figure 8) [11,34,41]

Both structure type share the same opening of the G- to H-ring followed by several water losses as demonstrated by the *m/z* 429.2636 and 411.2530 for the H- to M-side of the molecule. In accordance with Sibat et al, [34] and Suzuki et al., [41] the two characteristic ions of the CTXs: *m/z* 155.1067 and 125.0960 resulting from the opening of K-, L- and M-rings were detected in all three fragmentation spectra. Such fragmentation was not observed in CTX1B due to presence of the hydroxyl group on the M-ring.

The molecular formula of observed ions and the associated errors compared to theoretical monoisotopic mass are presented in Table 4.

The fragmentation spectra of CTX4A (Figure 8A and Table 4) presented two previously unreported ions, *m/z* 207.1370 (-4.8 ppm) corresponding to the opening of the K- ring and *m/z* 119.0863 (+6.7 ppm) originating from the opening of K- and L- ring followed by one water loss also present in two others spectra (Figure 8B and C).

For M-*seco*-CTX4A (Figure 8B), the opening of the J- and K- ring yielded in the formation of the *m/z* 237.1418 (-3.0 ppm).

As for the isomer (4) of CTX3C, the small difference in terms of retention time between the putative isomer of CTX4A (9.8 min, Figure S8) compared to the one of CTX4A (10.7 min, Figure S9) and the one of M-*seco*-CTX4A (5.2 min, Figure S4) suggest only a small difference on the structure as the compound eluted only 0.9 min earlier than CTX4A. No difference was found between targeted HRMS/MS spectra of CTX4A and the isomer of CTX4A (Figure 8A and C) pointing out that the difference between the two compound is potentially only related to a difference of a position of functional group within the structure.

553 Unfortunately, as the compound was only present at low amount in the sample, a potential in-
554 source water loss could be identified on the full scan spectra (Figure S8). More analysis on a
555 purified (or a more concentrated) sample will be required to determine the isomerism
556 relationship between the isomer of CTX4A and CTX4A.

557

558 **Table 4.** Ion species corresponding to the accurate mono-isotopic *m/z* of CTX4A, M-*seco*-CTX4A and isomer of
559 CTX4A. Mass differences (Δppm) were compared between theoretical exact mass and measured *m/z*.

Ion Formula	Theoretical mono isotopic mass (Da)	CTX4A	Δ ppm	M-*seco*-CTX4A	Δ ppm	Isomer of CTX4A	Δ ppm
$[C_{60}H_{85}O_{16}]^+$	1061,5832	1061,5683	-14,0	1061,5775	-5,4	1061,588	4,5
$[C_{60}H_{83}O_{15}]^+$	1043,5726	1043,5685	-3,9	1043,5634	-8,8	1043,5705	-2,0
$[C_{60}H_{81}O_{14}]^+$	1025,5621	1025,5572	-4,8	1025,5571	-4,9	1025,5564	-5,6
$[C_{60}H_{79}O_{13}]^+$	1007,5515	1007,55	-1,5	1007,543	-8,4	1007,5464	-5,1
$[C_{60}H_{77}O_{12}]^+$	989,541	989,5448	3,8	989,5348	-6,3	989,5375	-3,5
$[C_{26}H_{37}O_5]^+$	429,2636	429,2594	-9,8	429,2594	-9,8	429,2594	-9,8
$[C_{26}H_{35}O_4]^+$	411,253	411,2518	-2,9			411,2518	-2,9
$[C_{14}H_{21}O_3]^+$	237,1485			237,1478	-3,0		
$[C_{13}H_{18}O_2]^+$	207,138	207,137	-4,8			207,137	
$[C_9H_{15}O_2]^+$	155,1067	155,1068	0,6	155,1065	-1,3	155,1072	3,2
$[C_8H_{13}O]^+$	125,0961	125,0962	0,8	125,0958	-2,4	125,096	-0,8
$[C_8H_{11}]^+$	119,0855	119,0863	6,7	119,0863	6,7	119,0855	0,0
$[C_6H_{11}O]^+$	99,0804					99,0795	-9,1

560

561

562 ## 4. Conclusions

563 This study demonstrated the benefits of using a time- and cost-saving fractional factorial
564 design of experiment to assess the significance of HRMS ionization and ion transmission
565 parameters in order to improve the sensitivity for the detection of algal polyethers. It was a
566 first step towards a better understanding of their behavior in an electrospray source and in the
567 dual ion funnel that led to lowering their limits of detection. The increase of sensitivity
568 contributed to obtain higher-quality MS/MS fragmentation, which ultimately provided more
569 relevant structural information on ciguatoxin-like compounds. The toxin profile of
570 *G. polynesiensis* strain TB92 was re-described using high resolution mass spectrometry

resulting in the report of 44-methylgambierone produced at 50 times higher level than gambierone, the confirmation based on Full Scan and targeted MS/MS analysis of the presence of M-*seco*-CTX4A and the report of a putative isomer of CTX4A. For the first time, the signal enhancement in HRMS allowed for the acquisition of MS/MS spectra for CTX3B, 2-OH-CTX3C, the isomer (4) of CTX3C, CTX4A, M-*seco*-CTX4A and an isomer of CTX4A. Their structural comparison resulted in the report of constitutional isomerism for both type of isomers with a difference in the position of likely a methyl- or hydroxyl-group with no clear difference in the fragmentation pattern using MS^2. The perspective for the structural elucidation of the two isomers relies on the use of MS^n mass spectrometry or NMR spectroscopy on the purified compound.

Acknowledgements

This work was supported by Interreg Alertox-Net EAPA-317-2016. The PhD of Thomas Yon was funded by Ifremer (Contract-Reference n° 18/2 216 776F) and the Regional Council of the Pays de la Loire (convention - n° 2018-09813).

References

[1] R.J. Lewis, I. Vetter, Ciguatoxin and ciguatera, marine and freshwater toxins, Springer Netherlands, Dordrecht, (2015), 1-19. https://doi.org/10.1007/978-94-007-6650-1_13-1

[2] M.A. Friedman, M. Fernandez, L.C. Backer, R.W. Dickey, J. Bernstein, K. Schrank, S. Kibler, W. Stephan, M.O. Gribble, P. Bienfang, R.E. Bowen, S. Degrasse, H.A. Flores Quintana, C.R. Loeffler, R. Weisman, D. Blythe, E. Berdalet, R. Ayyar, D. Clarkson-Townsend, K. Swajian, R. Benner, T. Brewer, L.E. Fleming, An updated review of ciguatera fish poisoning: clinical, epidemiological, environmental, and public health management, Marine Drugs 15, (2017), 72 .https://dx.doi.org/10.3390/md15030072

[3] M. Chinain, C.M.i. Gatti, H.T. Darius, J.P. Quod, P.A. Tester, Ciguatera poisonings: a global review of occurrences and trends, Harmful Algae (2020) , https://doi.org/10.1016/j.hal.2020.101873

[4] R. Bagnis, S. Chanteau, E. Chungue, J.M. Hurtel, T. Yasumoto , A. Inoue, Origins of ciguatera fish poisoning: a new dinoflagellate, *Gambierdiscus toxicus* Adachi and Fukuyo, definitively involved as a causal agent, Toxicon 18 (1980), 2, 199-208 https://doi.org/10.1016/0041-0101(80)90074-4

[5] F. Pisapia, W.C. Holland, D.R. Hardison, R.W. Litaker, S. Fraga, T. Nishimura, M. Adachi, L. Nguyen-Ngoc, V. Séchet, Z. Amzil, C. Herrenknecht, P. Hess, Toxicity screening of 13 *Gambierdiscus* strains using neuro-2a and erythrocyte lysis bioassays, Harmful Algae, 63, (2017), 173-183. http://dx.doi.org/10.1016/j.hal.2017.02.005

[6] R. Munday, S. Murray, L.L. Rhodes, M.E. Larsson, D.T. Harwood, Ciguatoxins and maitotoxins in extracts of sixteen *Gambierdiscus* isolates and one *Fukuyoa* isolate from the South Pacific and their toxicity to mice by intraperitoneal and oral administration, Marine Drugs, 15, (2017), 10. https://doi.org/10.3390/md15070208

[7] L. Reverté, A. Toldrà, K.B. Andree, S. Fraga, G. de Falco, M. Campàs, J. Diogène, Assessment of cytotoxicity in ten strains of *Gambierdiscus australes* from Macaronesian Islands by neuro-2a cell-based assays, Journal of Applied Phycology 30, (2018), 2447-2461 . https://doi.org/10.1007/s10811-018-1456-8

[8] S. Longo, M. Sibat, J. Viallon, H.T. Darius, P. Hess, M. Chinain, Intraspecific variability in the toxin production and toxin profiles of in vitro cultures of *Gambierdiscus polynesiensis* (Dinophyceae) from French Polynesia, Toxins, 11, (2019) 735. https://doi.org/10.3390/toxins11120735

[9] R.W. Litaker, W.C. Holland, D.R. Hardison, F. Pisapia, P. Hess, S.R. Kibler, P.A. Tester, Ciguatoxicity of *Gambierdiscus* and *Fukuyoa* species from the Caribbean and Gulf of Mexico, PLoS One, 12, (2017). https://doi.org/10.1371/journal.pone.0185776

[10] M. Chinain, M.A. Faust, S. Pauillac, Morphology and molecular analyses of three toxic species of *Gambierdiscus* (Dinophyceae): *G. pacificus*, sp. nov., *G. australes*, sp. nov., and *G. polynesiensis*, sp. nov., Journal of Phycology, 35, (1999), 1282-1296. https://doi.org/10.1046/j.1529-8817.1999.3561282.x

[11] M. Chinain, H.T. Darius, A. Ung, P. Cruchet, Z. Wang, D. Ponton, D. Laurent, S. Pauillac, Growth and toxin production in the ciguatera-causing dinoflagellate *Gambierdiscus polynesiensis* (Dinophyceae) in culture, Toxicon, 56, (2010), 739-750.http:/dx.doi.org/10.1016/j.toxicon.2009.06.013

[12] L. Rhodes, T. Harwood, K. Smith, P. Argyle, R. Munday, Production of ciguatoxin and maitotoxin by strains of *Gambierdiscus australes*, *G. pacificus* and *G. polynesiensis* (Dinophyceae) isolated from Rarotonga, Cook Islands, Harmful Algae 39, (2014), 185-190. http://dx.doi.org/10.1016/j.hal.2014.07.018

[13] M. Satake, T. Yasumoto, Methods for determining the absolute configurations of marine ladder-shaped polyethers, Chirality 32, (2020), 474-483. https://doi.org/10.1002/chir.23187

[14] M. Murata, H. Naoki, T. Iwashita, S. Matsunaga, M. Sasaki, A. Yokoyama, T. Yasumoto, Structure of maitotoxin, Journal of the American Chemical Society, 115, (1993), 2060-2062. https://doi.org/10.1021/ja00058a075

[15] R.J. Lewis, M. Inserra, I. Vetter, W.C. Holland, D.R. Hardison, P.A. Tester, R.W. Litaker, Rapid extraction and identification of maitotoxin and ciguatoxin-like toxins from Caribbean and Pacific *Gambierdiscus* using a new functional bioassay, PloS one, 11, (2016). https://doi.org/10.1371/journal.pone.0160006

[16] F. Pisapia, M. Sibat, C. Herrenknecht, K. Lhaute, G. Gaiani, P.J. Ferron, V. Fessard, S. Fraga, S.M. Nascimento, R.W. Litaker, W.C. Holland, C. Roullier, P. Hess, Maitotoxin-4, a novel MTX analog produced by *Gambierdiscus excentricus*, Marine Drugs, 15, (2017), 31. https://doi.org/10.3390/md15070220

[17] E.P. Mazzola, J.R. Deeds, W.L. Stutts, C.D. Ridge, R.W. Dickey, K.D. White, R.T. Williamson, G.E. Martin, Elucidation and partial NMR assignment of monosulfated maitotoxins from the Caribbean, Toxicon, 164, (2019), 44-50. https://doi.org/10.1016/j.toxicon.2019.03.026

[18] H. Nagai, K. Torigoe, M. Satake, M. Murata, T. Yasumoto, H. Hirota, Gambieric acids: unprecedented potent antifungal substances isolated from cultures of a marine dinoflagellate *Gambierdiscus toxicus*, Journal of the American Chemical Society, 114, (1992), 1102-1103. https://doi.org/10.1021/Ja00029a057

[19] H. Nagai, M. Murata, K. Torigoe, M. Satake, T. Yasumoto, Gambieric acids, new potent antifungal substances with unprecedented polyether structures from a marine dinoflagellate *Gambierdiscus toxicus*, Journal of Organic Chemistry, 57, (1992), 5448-5453. https://doi.org/10.1021/jo00046a029

[20] R. Watanabe, H. Uchida, T. Suzuki, R. Matsushima, M. Nagae, Y. Toyohara, M. Satake, Y. Oshima, A. Inoue, T. Yasumoto, Gambieroxide, a novel epoxy polyether compound from the dinoflagellate *Gambierdiscus toxicus* GTP2 strain, Tetrahedron, 69, (2013), 10299-10303. https://doi.org/10.1016/j.tet.2013.10.022

[21] M. Satake, M. Murata, T. Yasumoto, Gambierol - a new toxic polyether compound isolated from the marine dinoflagellate *Gambierdiscus toxicus*, Journal of the American Chemical Society, 115, (1993), 361-362. https://doi.org/10.1021/ja00054a061

[22] I. Rodriguez, G. Genta-Jouve, C. Alfonso, K. Calabro, E. Alonso, J.A. Sanchez, A. Alfonso, O.P. Thomas, L.M. Botana, Gambierone, a ladder-shaped polyether from the dinoflagellate *Gambierdiscus belizeanus*, Organic Letters, 17, (2015), 2392-2395. https://doi.org/10.1021/acs.orglett.5b00902

[23] A. Boente-Juncal, M. Alvarez, A. Antelo, I. Rodriguez, K. Calabro, C. Vale, O.P. Thomas, L.M. Botana, Structure elucidation and biological evaluation of maitotoxin-3, a homologue of gambierone, from *Gambierdiscus belizeanus*, Toxins, 11, (2019), 19. https://doi.org/10.3390/toxins11020079

[24] J.S. Murray, A.I. Selwood, D.T. Harwood, R. van Ginkel, J. Puddick, L.L. Rhodes, F. Rise, A.L. Wilkins, 44-Methylgambierone, a new gambierone analogue isolated from *Gambierdiscus australes*, Tetrahedron Letters, 60, (2019), 621-625. https://doi.org/10.1016/j.tetlet.2019.01.043

[25] C.E.J.d.A. Tibiriçá, M. Sibat, L.F. Fernandes, G. Bilien, N. Chomérat, P. Hess, L.L. Mafra Jr, Diversity and toxicity of the genus *Coolia Meunier* in Brazil, and detection of 44-methyl gambierone in *Coolia tropicalis*, Toxins, 12, (2020), 327. https://doi.org/10.3390/toxins12050327

[26] J.S. Murray, T. Nishimura, S.C. Finch, L.L. Rhodes, J. Puddick, D.T. Harwood, M.E. Larsson, M.A. Doblin, P. Leung, M. Yan, F. Rise, A.L. Wilkins, M.R. Prinsep, The role of 44-methylgambierone in ciguatera fish poisoning: acute toxicity, production by marine microalgae and its potential as a biomarker for *Gambierdiscus spp*, Harmful Algae, 97, (2020), 8. https://doi.org/10.1016/j.hal.2020.101853

[27] P. Estevez, M. Sibat, J. Leão-Martins, À. Tudó, M. Rambla-Alegre, K. Aligizaki, J. Diogène, A. Gago-Martinez, P. Hess, Use of mass spectrometry to determine the diversity of toxins produced by *Gambierdiscus* and *Fukuyoa* species from Balearic Islands and Crete (Mediterranean Sea) and the Canary Islands (Northeast Atlantic), Toxins, 12, (2020), 305. https://doi.org/10.3390/toxins12050305

[28] National Center for Biotechnology Information (2020). PubChem Compound Summary. https://pubchem.ncbi.nlm.nih.gov. (Accessed December 2020).

[29] L. Solino, P.R. Costa, Differential toxin profiles of ciguatoxins in marine organisms: chemistry, fate and global distribution, Toxicon, 150, (2018), 124-143. https://doi.org/10.1016/j.toxicon.2018.05.005

[30] EFSA panel on contaminants in the food chain, scientific opinion on marine biotoxins in shellfish – Emerging toxins: ciguatoxin group, EFSA Journal, 8, (2010), 1627. https://doi.org/10.2903/j.efsa.2010.1627

[31] T. Yasumoto, T. Igarashi, A.-M. Legrand, P. Cruchet, M. Chinain, T. Fujita, H. Naoki, Structural elucidation of ciguatoxin congeners by fast-atom bombardment tandem mass spectroscopy, Journal of American Chemical Society, 122, (2000), 4988-4989. https://doi.org/10.1021/ja9944204

[32] M. Roue, H.T. Darius, S. Picot, A. Ung, J. Viallon, N. Gaertner-Mazouni, M. Sibat, Z. Amzil, M. Chinain, Evidence of the bioaccumulation of ciguatoxins in giant clams (*Tridacna maxima*) exposed to *Gambierdiscus spp*. cells, Harmful Algae, 57, (2016), 78-87. https://doi.org/10.1016/j.hal.2016.05.007

[33] J.S. Murray, M.J. Boundy, A.I. Selwood, D.T. Harwood, Development of an LC-MS/MS method to simultaneously monitor maitotoxins and selected ciguatoxins in algal cultures and P-CTX-1B in fish, Harmful Algae, 80, (2018), 80-87. https://doi.org/10.1016/j.hal.2018.09.001

[34] M. Sibat, C. Herrenknecht, H.T. Darius, M. Roué, M. Chinain, P. Hess, Detection of pacific ciguatoxins using liquid chromatography coupled to either low or high resolution mass spectrometry (LC-MS/MS), Journal of Chromatography A, 1571, (2018), 16-28. https://doi.org/10.1016/j.chroma.2018.08.008

[35] FAO and WHO, Report of the expert meeting on ciguatera poisoning. Rome, 19–23 November 2018, Food Safety and Quality No. 9. Rome. (2020). https://doi.org/10.4060/ca8817en

[36] T. Yasumoto, The chemistry and biological function of natural marine toxins, Chemical Record, 1, (2001), 228-242. https://doi.org/10.1002/tcr.1010

[37] M. Roue, H.T. Darius, J. Viallon, A. Ung, C. Gatti, D.T. Harwood, M. Chinain, Application of solid phase adsorption toxin tracking (SPATT) devices for the field detection of *Gambierdiscus* toxins, Harmful Algae, 71, (2018), 40-49. https://doi.org/10.1016/j.hal.2017.11.006

[38] S. Longo, M. Sibat, H.T. Darius, P. Hess, M. Chinain, Effects of pH and nutrients (nitrogen) on growth and toxin profile of the ciguatera-causing dinoflagellate *Gambierdiscus polynesiensis* (Dinophyceae), Toxins, 12, (2020), 767. https://doi.org/10.3390/toxins12120767

[39] P.A. Argyle, D.T. Harwood, L.L. Rhodes, O. Champeau, L.A. Tremblay, Toxicity assessment of New Zealand and Pacific dinoflagellates *Ostreopsis* and *Gambierdiscus* (Dinophyceae) extracts using bioassays, New Zealand Journal of Marine and Freshwater Research, 50, (2016), 444-456. https://doi.org/10.1080/00288330.2016.1159581

[40] M. Roué, K.F. Smith, M. Sibat, J. Viallon, K. Henry, A. Ung, L. Biessy, P. Hess, H.T. Darius, M. Chinain, Assessment of ciguatera and other phycotoxin-related risks in Anaho Bay (Nuku Hiva Island, French Polynesia): molecular, toxicological, and chemical analyses of passive samplers, Toxins, 12, (2020), 321. https://doi.org/10.3390/toxins12050321

[41] T. Suzuki, D.V. Ha, A. Uesugi, H. Uchida, Analytical challenges to ciguatoxins, Current Opinion in Food Science, 18, (2017), 37-42. https://doi.org/10.1016/j.cofs.2017.10.004

[42] G. Moreiras, J.M. Leao, A. Gago-Martinez, Design of experiments for the optimization of electrospray ionization in the LC-MS/MS analysis of ciguatoxins, Journal of mass spectrometry, 53, (2018), 1059-1069. https://doi.org/10.1002/jms.4281

[43] G. Orellana, J. Vanden Bussche, L. Van Meulebroek, M. Vandegehuchte, C. Janssen, L. Vanhaecke, Validation of a confirmatory method for lipophilic marine toxins in shellfish using UHPLC-HR-Orbitrap MS, Analytical and Bioanalytical Chemistry, 406, (2014), 5303-5312. https://doi.org/10.1007/s00216-014-7958-6

[44] A.J.C. Andersen, L.S. de Medeiros, S.B. Binzer, S.A. Rasmussen, P.J. Hansen, K.F. Nielsen, K. Jorgensen, T.O. Larsen, HPLC-HRMS quantification of the ichthyotoxin karmitoxin from *Karlodinium armiger*, Marine Drugs, 15, (2017), 278. https://doi.org/10.3390/md15090278

[45] K. Yogi, N. Oshiro, Y. Inafuku, M. Hirama, T. Yasumoto, Detailed LC-MS/MS analysis of ciguatoxins revealing distinct regional and species characteristics in fish and causative alga from the Pacific, Analytical Chemistry, 83, (2011), 8886-8891. https://doi.org/10.1021/ac200799j

[46] M.D. Peris-Diaz, O. Rodak, S.R. Sweeney, A. Krezel, E. Sentandreu, Chemometrics-assisted optimization of liquid chromatography-quadrupole-time-of-flight mass spectrometry analysis for targeted metabolomics, Talanta, 199, (2019), 380-387. https://doi.org/10.1016/j.talanta.2019.02.075

[47] Agilent, Agilent Q-TOF LC/MS Techniques & Operation for Small Molecules, student manual volume I, II and III, 2018.

[48] Agilent, Agilent 6200 series TOF and 6500 series Q-TOF LC/MS system concepts guide, 2014.

[49] R.N. Mead, E.E. Probst, J.R. Helms, G.B. Avery, R.J. Kieber, S.A. Skrabal, Enhanced detection of the algal toxin PbTx-2 in marine waters by atmospheric pressure chemical ionization mass spectrometry, Rapid Communications in Mass Spectrometry, 28, (2014), 2455-2460. https://doi.org/10.1002/rcm.7032

[50] R.T. Kelly, A.V. Tolmachev, J.S. Page, K.Q. Tang, R.D. Smith, The ion funnel: theory, implementations, and applications, Mass Spectrometry Reviews, 29, (2010), 294-312. https://doi.org/10.1002/mas.20232

[51] D.A. Volmer, C.M. Lock, Electrospray ionization and collision-induced dissociation of antibiotic polyether ionophores, Rapid Communications in Mass Spectrometry, 12, (1998), 157-164. https://doi.org/10.1002/(SICI)1097-0231(19980227)12:4<157::AID-RCM134>3.0.CO;2-M

[52] M. Roué, H. Darius, A. Ung, J. Viallon, M. Sibat, P. Hess, Z. Amzil, M. Chinain, Tissue distribution and elimination of ciguatoxins in *Tridacna maxima* (Tridacnidae, Bivalvia) fed *Gambierdiscus polynesiensis*, Toxins, 10, (2018), 189. https://doi.org/10.3390/toxins10050189

[53] S.H. Jang, H.J. Jeong, Y.D. Yoo, *Gambierdiscus jejuensis* sp. nov., an epiphytic dinoflagellate from the waters of Jeju Island, Korea, effect of temperature on the growth, and its global distribution, Harmful Algae, 80, (2018), 149-157. https://doi.org/10.1016/j.hal.2018.11.007

[54] L. Patiny, A. Borel, ChemCalc: a building block for tomorrow's chemical infrastructure, Journal of Chemical Information and Modeling, 53, (2013), 1223-1228. https://doi.org/10.1021/ci300563h

[55] R.J. Lewis, R.S. Norton, I.M. Brereton, C.D. Eccles, Ciguatoxin-2 is a diastereomer of ciguatoxin-3, Toxicon 31, (1993) 637-643. https://doi.org/10.1016/0041-0101(93)90118-3

Highlights :

- A chemometric method to weigh the contribution of Q-TOF parameters is proposed
- Ionization and transmission parameter increased sensitivity for ciguatoxin analysis
- M-*seco*-P-CTX4A is a major ciguatoxin produced by *G. polynesiensis*
- Putatively reported “isomer (4) of P-CTX3C” is a constitutional isomer

Authors

Thomas Yon[1], Manoella Sibat[1], Damien Réveillon[1], Samuel Bertrand[2,3], Mireille Chinain[4], Philipp Hess[1]

[1] IFREMER, DYNECO, Laboratoire Phycotoxines, F-44000 Nantes, France

[2] Université de Nantes, MMS, EA 2160, Nantes, France.

[3] ThalassOMICS Metabolomics Facility, Plateforme Corsaire, Biogenouest, Nantes, France.

[4] Institut Louis Malardé, UMR 241 EIO, 98713 Papeete, Tahiti, French Polynesia

Corresponding author: Thomas Yon Thomas.yon@ifremer.fr

Declaration of interests

☒ The authors declare that they have no known competing financial interests or personal relationships that could have appeared to influence the work reported in this paper.